

Synthesis, characterization and theoretical study of a new liquid crystal compound with an oxazepine core



AbdulKarim-Talaq Mohammad^{a,*}, Guan-Yeow Yeap^b, Hasnah Osman^b

^aChemistry Department, College of Science, Anbar University, Ramadi, Iraq

^bLiquid Crystal Research Laboratory, School of Chemical Sciences, Universiti Sains Malaysia, Minden 11800, Penang, Malaysia

HIGHLIGHTS

- A novel heterocyclic compounds based liquid crystal were synthesized and identified.
- The relationship of the core structures and the mesomorphic were investigated.
- Theoretical studies was studied.
- The SmA and N phases were observed.
- The nematic phase can only observed in long-chain derivatives.

ARTICLE INFO

Article history:

Received 9 September 2014
Received in revised form 22 December 2014
Accepted 23 January 2015
Available online 3 February 2015

Keywords:

Oxazepine
SmA
N phases

ABSTRACT

A novel synthesis of heterocyclic liquid crystal compounds containing a seven-membered 1,3-oxazepine with terminal alkyloxy chains has been carried out. The molecular structures of these compounds were substantiated by FT-IR NMR elemental analysis. The relationship between the structures and the mesomorphic behaviours of their derivatives were investigated. The results showed that the formation of mesophases is strongly dependent on the type of core moiety. All compounds with oxazepinediones and oxazepanediones are non-mesogenic and only exhibit Cr₁–Cr₂ upon cooling and heating. However, the SmA and N phases were observed in the 5,6-benzo [1,3] oxazepine-4,7-diones series of compounds. The study also revealed that the length of the alkyl chain has a significant effect on the liquid crystalline properties; the nematic phase can only observed in long-chain derivatives of 5,6-benzo [1,3] oxazepine-4,7-diones. Theoretical studies are in agreement with our result.

Published by Elsevier B.V.

Introduction

Liquid–crystal synthesis has been investigated due to the successful development and application of liquid crystals, particularly in the area of electro-optical display [1]. In recent decades there has been much interest in the synthesis and characterization of heterocyclic compounds because of their interesting properties, such as liquid–crystallinity and nonlinear optical properties [2–6]. Among these materials, disk-like liquid crystals are particularly worthy of attention [7–10]. Liquid crystalline materials are of great interest, especially because of their unique optical properties. The ability of liquid crystalline phases to regulate reactivity depends on a number of factors, such as the mesophase type and reactant molecular length, flexibility and polarizability [11]. For this reason,

altering the core structure is a significant factor that changes the mesomorphic properties [12]. Heterocycles are of great importance as core units in thermotropic liquid crystals because they can impart lateral and/or longitudinal dipoles combined with changes in the molecular shape [13,14]. The incorporation of heteroatoms result in considerable changes in the corresponding liquid crystalline phases and/or in the physical properties of the observed phases, as most of the heteroatoms (S, O, and N) commonly introduced are more polarizable than carbon [15]. We recently reported the synthesis and characterization of a large number of three type-ring heterocyclic oxazepine LC materials that exhibited one phase, N (nematic) phase [16–18]. This work was one of the first to report the incorporation of the oxazepine moiety in a mesogen structure and clearly demonstrated that this moiety is conducive to the formation of the tilted nematic phase. In a continuation of our work on oxazepine-based mesogen compounds, we will describe the thermal and electro-optic results obtained from the three series of compounds containing the oxazepindione moiety. The phase

* Corresponding author. Tel.: +964 7902529959, +1 330 3895376.

E-mail addresses: drmohamadtaaq@gmail.com, mtalaq_gst@kent.edu (A.K.-T. Mohammad).

transition temperatures and enthalpy values of the title compounds were measured by differential scanning calorimetry (DSC), and the textures of the mesophases were studied using a polarizing optical microscope (POM). The physical properties of the title compounds were studied by Fourier transform infrared (FT-IR) and high resolution nuclear magnetic resonance NMR (^1H and ^{13}C NMR).

Experimental

Maleic anhydride, succinic anhydride, phthalic anhydride, 4-hydroxybenzaldehyde, 4-hydroxyaniline, 1-bromohexane, 1-bromooctane, 1-bromodecane, 1-bromododecane, 1-bromohexadecane and 1-bromooctadecane (Aldrich), 1-bromotetradecane (Merch), were used directly without further purification. Thin-layer chromatography (TLC) was performed on silica-gel plates.

Synthesis

The synthetic routes toward formation of all the title compounds with numbering atom are depicted in Scheme 1. The synthesis of each compound in the series was identical.

4-(4-hydroxybenzylideneamino)phenol

The imine was synthesized by mixing equimolar amounts of 4-hydroxybenzaldehyde with *p*-hydroxyaniline in absolute ethanol. The reaction mixture was refluxed for 2 h. The solution was then allowed to cool to room temperature which formed a precipitate that was filtered. The filter cake was crystallized from absolute ethanol and dried under reduced pressure.

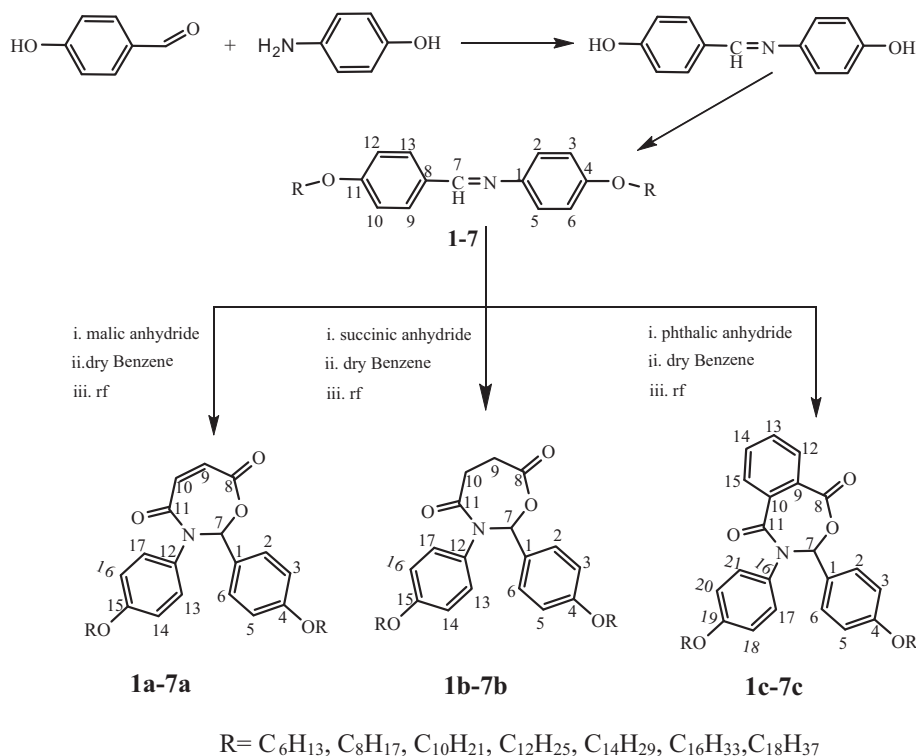
General procedure for the synthesis of 4-(alkyloxy)-*N*-(4-(alkyloxy)benzylidene)aniline (1-7)

The compounds were synthesized by the same method as described for compound 1.

A mixture containing 0.1 mol of 4-(4-hydroxybenzylideneamino)phenol, 0.25 mol of anhydrous sodium carbonate and 0.25 mol of 1-bromohexane was dissolved in 50 mL of DMF and allowed to heat for 4 h at 150 °C under continuous stirring as documented by Yeap et al. [16]. The resulting mixture was then poured into an ice-water bath (approx. 5 °C) whereupon a precipitate formed. The precipitate was filtered and washed once with KOH and water, dried and finally recrystallized from ethanol to yield compound 1 in 77% yield.

The yields, elemental analytical, select FT-IR, ^1H and ^{13}C NMR data for compounds 1-7 are summarized as follows:

- Yield 77%; m.p. 80–81 °C. Anal. found for $\text{C}_{25}\text{H}_{35}\text{NO}_2$ (%): C 78.90, H 9.18, N 3.60. Calc (%) C 78.70, H 9.25, N 3.67. IR: ν_{max} (cm^{-1}): 3055, 2980, 2951, 1620, 1610, 1580, 1250. ^1H NMR δ (ppm): 7.70 (d, H2 and H6), 7.31 (d, H3 and H5), 8.51 (s, H7), 7.19 (d, H9 and H13), 7.08 (d, H10 and H12), 4.12 (t, $\text{C}_4\text{—OCH}_2$), 4.01 (t, $\text{C}_{11}\text{—OCH}_2$), 1.87–1.21 (m, $(\text{CH}_2)_n$), 0.80 (t, CH_3). ^{13}C NMR δ (ppm): 115.11–133.12 (Ar—C), 161.11 (Ar—C—O), 164.23 (C=N), 70.03 (O— CH_2), 22.32–32.88 (CH_2) $_n$, 15.04 (CH_3).
- Yield 85 %; m.p. 83–84 °C. Anal. found for $\text{C}_{29}\text{H}_{43}\text{NO}$ (%): C 79.64, H 9.78, N 3.12. Calc (%) C 79.59, H 9.90, N 3.20. IR: ν_{max} (cm^{-1}): 3054, 2985, 2950, 1625, 1604, 1583, 1247. ^1H NMR δ (ppm): 7.72 (d, H2 and H6), 7.30 (d, H3 and H5), 8.47 (s, H7), 7.15 (d, H9 and H13), 7.05 (d, H10 and H12), 4.11 (t, $\text{C}_4\text{—OCH}_2$), 4.02 (t, $\text{C}_{11}\text{—OCH}_2$), 1.80–1.20 (m, $(\text{CH}_2)_n$), 0.82 (t, CH_3). ^{13}C NMR δ (ppm): 115.55–132.89 (Ar—C), 161.55 (Ar—C—O), 164.61 (C=N), 70.51 (O— CH_2), 22.81–32.02 (CH_2) $_n$, 15.17 (CH_3).
- Yield 72 %; m.p. 87–88 °C. Anal. found for $\text{C}_{33}\text{H}_{51}\text{NO}_2$ (%): C 80.35, H 10.33, N 2.90. Calc (%) C 80.27, H 10.41, N 2.84. IR: ν_{max} (cm^{-1}): 3052, 2982, 2952, 1628, 1607, 1580, 1252. ^1H NMR δ (ppm): 7.71 (d, H2 and H6), 7.31 (d, H3 and H5), 8.52 (s, H7), 7.14 (d, H9 and H13), 7.02 (d, H10 and H12), 4.10 (t, $\text{C}_4\text{—OCH}_2$), 4.02 (t, $\text{C}_{11}\text{—OCH}_2$), 1.82–1.26 (m, $(\text{CH}_2)_n$), 0.87 (t, CH_3). ^{13}C NMR δ (ppm): 115.80–132.06 (Ar—C), 161.01 (Ar—C—O), 164.40 (C=N), 70.77 (O— CH_2), 23.20–32.71 (CH_2) $_n$, 15.81 (CH_3).



Scheme 1. Synthetic route to synthesis title compounds 1a-7a, 1b-7b and 1c-7c.

Table 1
Physical and analytical data of compounds **1a–7a**, **1b–7b** and **1c–7c**.

Compounds	Yield %	Molecular formula	Elemental analysis %, found (calculated)		
			C	H	N
1a	70	C ₂₉ H ₃₇ NO ₅	72.45 (72.62)	7.84 (7.78)	2.97 (2.92)
2a	66	C ₃₃ H ₄₅ NO ₅	73.80 (73.99)	8.33 (8.47)	2.74 (2.61)
3a	63	C ₃₇ H ₅₃ NO ₅	75.15 (75.09)	9.19 (9.03)	2.28 (2.37)
4a	55	C ₄₁ H ₆₁ NO ₅	76.11 (76.00)	9.37 (9.49)	2.25 (2.16)
5a	59	C ₄₅ H ₆₉ NO ₅	76.86 (76.77)	9.74 (9.88)	1.91 (1.99)
6a	64	C ₄₉ H ₇₇ NO ₅	77.52 (77.42)	10.31 (10.21)	1.92 (1.84)
7a	59	C ₅₃ H ₈₅ NO ₅	77.83 (77.99)	10.62 (10.50)	1.79 (1.72)
1b	60	C ₂₉ H ₃₉ NO ₅	72.50 (72.32)	8.23 (8.16)	2.98 (2.91)
2b	62	C ₃₃ H ₄₇ NO ₅	73.66 (73.71)	8.84 (8.81)	2.57 (2.60)
3b	60	C ₃₇ H ₅₅ NO ₅	74.79 (74.83)	9.41 (9.34)	2.29 (2.36)
4b	67	C ₄₁ H ₆₃ NO ₅	75.85 (75.77)	9.66 (9.77)	2.20 (2.16)
5b	69	C ₄₅ H ₇₁ NO ₅	76.42 (76.55)	10.06 (10.14)	1.83 (1.98)
6b	64	C ₄₉ H ₇₉ NO ₅	77.30 (77.22)	10.29 (10.45)	1.72 (1.84)
7b	57	C ₅₃ H ₈₇ NO ₅	77.92 (77.80)	10.89 (10.72)	1.78 (1.71)
1c	58	C ₃₃ H ₃₉ NO ₅	74.69 (74.83)	7.57 (7.42)	2.70 (2.64)
2c	52	C ₃₇ H ₄₇ NO ₅	75.90 (75.86)	8.17 (8.09)	2.51 (2.39)
3c	56	C ₄₁ H ₅₅ NO ₅	76.60 (76.72)	8.80 (8.64)	2.25 (2.18)
4c	66	C ₄₅ H ₆₃ NO ₅	77.65 (77.43)	9.24 (9.10)	2.17 (2.01)
5c	51	C ₄₉ H ₇₁ NO ₅	78.12 (78.04)	9.58 (9.49)	1.80 (1.86)
6c	54	C ₅₃ H ₇₉ NO ₅	78.40 (78.57)	9.77 (9.83)	1.54 (1.73)
7c	48	C ₅₇ H ₈₇ NO ₅	79.20 (79.03)	10.28 (10.12)	1.74 (1.62)

4. Yield 74%; m.p. 91–92 °C. Anal. found for C₃₇H₅₉NO₂ (%): C 80.66, H 10.77, N 2.50. Calc (%) C 80.82, H 10.82, N 2.55. IR: ν_{\max} (cm⁻¹): 3055, 2986, 2950, 1622, 1604, 1585, 1240. ¹H NMR δ (ppm): 7.70 (d, H2 and H6), 7.32 (d, H3 and H5), 8.61 (s, H7), 7.13 (d, H9 and H13), 7.01 (d, H10 and H12), 4.13 (t, C₄—OCH₂), 4.00 (t, C₁₁—OCH₂), 1.83–1.24 (m, (CH₂)_n), 0.88 (t, CH₃). ¹³C NMR δ (ppm): 115.21–132.89 (Ar—C), 161.65 (Ar—C—O), 164.55 (C=N), 70.09 (O—CH₂), 23.38–32.09 (CH₂)_n, 15.41 (CH₃).
5. Yield 83%; m.p. 95–96 °C. Anal. found for C₄₁H₆₇NO₂ (%): C 81.09, H 11.21, N 2.22. Calc (%) C 81.26, H 11.14, N 2.31. IR: ν_{\max} (cm⁻¹): 3051, 2981, 2953, 1620, 1602, 1582, 1254. ¹H NMR δ (ppm): 7.73 (d, H2 and H6), 7.30 (d, H3 and H5), 8.59 (s, H7), 7.16 (d, H9 and H13), 7.00 (d, H10 and H12), 4.12 (t, C₄—OCH₂), 4.03 (t, C₁₁—OCH₂), 1.82–1.23 (m, (CH₂)_n), 0.86 (t, CH₃). ¹³C NMR δ (ppm): 115.66–132.34 (Ar—C), 161.67 (Ar—C—O), 164.23 (C=N), 70.23 (O—CH₂), 23.43–32.17 (CH₂)_n, 15.02 (CH₃).
6. Yield 78%; m.p. 99–100 °C. Anal. found for C₄₅H₇₅NO₂ (%): C 81.47, H 11.59, N 2.23. Calc (%) C 81.63, H 11.42, N 2.12. IR: ν_{\max} (cm⁻¹): 3055, 2983, 2952, 1628, 1601, 1588, 1248. ¹H NMR δ (ppm): 7.76 (d, H2 and H6), 7.35 (d, H3 and H5), 8.47 (s, H7), 7.12 (d, H9 and H13), 7.05 (d, H10 and H12), 4.11 (t, C₄—OCH₂), 4.00 (t, C₁₁—OCH₂), 1.83–1.24 (m, (CH₂)_n), 0.88 (t, CH₃). ¹³C NMR δ (ppm): 115.09–132.00 (Ar—C), 161.20 (Ar—C—O), 164.66 (C=N), 70.45 (O—CH₂), 23.81–32.79 (CH₂)_n, 15.00 (CH₃).
7. Yield 85%; m.p. 104–105 °C. Anal. found for C₄₉H₈₃NO₂ (%): C 81.79, H 11.75, N 1.90. Calc (%) C 81.95, H 11.65, N 1.95. IR: ν_{\max} (cm⁻¹): 3052, 2981, 2954, 1630, 1606, 1587, 1253. ¹H NMR δ (ppm): 7.72 (d, H2 and H6), 7.31 (d, H3 and H5), 8.55 (s, H7), 7.10 (d, H9 and H13), 7.03 (d, H10 and H12), 4.14 (t, C₄—OCH₂), 4.05 (t, C₁₁—OCH₂), 1.82–1.22 (m, (CH₂)_n), 0.89 (t, CH₃). ¹³C NMR δ (ppm): 116.34–132.87 (Ar—C), 161.66 (Ar—C—O), 164.17 (C=N), 70.81 (O—CH₂), 23.08–32.41 (CH₂)_n, 15.65 (CH₃).

Synthesis of compounds **1a–7a**, **1b–7b** and **1c–7c**

The title compounds were synthesized according to the method described by Yeap et al. and Tang et al. [17,19]. The synthetic method will be the same as described for compound **1a**.

Maleic anhydride (0.01 mol) was dissolved in dry benzene (10 mL) and added dropwise to a hot dry benzene solution (20 mL) containing compound **1** (0.01 mol) in a round bottom flask equipped with a double surface condenser fitted with a calcium chloride guard tube. The reaction mixture was refluxed for 2 h with

TLC monitoring. The solvent was distilled off in vacuo and the solid product thus obtained was filtered and washed with distilled cool water. The resulting solid was recrystallized twice from 1,4-dioxane. The physical and analytical data of **1a–7a**, **1b–7b** and **1c–7c** are listed in Table 1.

Techniques

The elemental (CHN) microanalyses were performed using a Perkin Elmer 2400 LS Series CHNS/O analyzer. Melting points were recorded on a Gallenkamp digital melting point instrument. FT-IR measurements on intermediates and title compounds were performed on samples in KBr pellets and the spectra recorded in the range of 4000–400 cm⁻¹ using a Perkin Elmer 2000-FT-IR spectrophotometer. The ¹H NMR and ¹³C NMR spectra were recorded in CDCl₃ (for **1–7**) and DMSO (for **1a–7b**, **1b–7b** and **1c–7c**) at 25 °C

Table 2
Phase transition temperatures (°C) and the corresponding enthalpies (J/g) of title compounds **1a–7a**, **1b–7b** and **1c–7c**.

Compounds	Transition temperature °C (corresponding enthalpy changes in kJ mol ⁻¹) heating/cooling
1a	Cr 128.18 (31.68) I Cr 71.20 (–28.34) I
2a	Cr 134.74 (68.11) I Cr 76.50 (–42.22) I
3a	Cr 139.26 (55.29) I Cr 84.48 (–17.69) I
4a	Cr 148.37 (25.69) I Cr 93.72 (–31.07) I
5a	Cr 144.23 (23.45) Cr ₂ 156.92 (28.17) I Cr 132.78 (–22.40) Cr ₂ 149.30 (–33.21) I
6a	Cr 147.61 (19.53) Cr ₂ 160.84 (34.07) I Cr 134.23 (–30.20) Cr ₂ 154.00 (–24.20) I
7a	Cr 151.20 (16.90) Cr ₂ 167.70 (40.00) I Cr 142.60 (–36.72) Cr ₂ 160.00 (–18.49) I
1b	Cr ₁ 65.19 (29.00) Cr ₂ 140.10 (80.23) I Cr ₁ 70.93 (–24.67) Cr ₂ 133.50 (–30.14) I
2b	Cr ₁ 81.10 (50.37) Cr ₂ 146.80 (30.24) I Cr ₁ 74.30 (–22.59) Cr ₂ 140.70 (–19.30) I
3b	Cr ₁ 94.34 (42.31) Cr ₂ 156.27 (13.70) I Cr ₁ 88.40 (–16.89) Cr ₂ 144.64 (–49.08) I
4b	Cr ₁ 87.30 (18.50) Cr ₂ 163.20 (20.57) I Cr ₁ 71.20 (–29.36) Cr ₂ 136.58 (–13.46) I
5b	Cr ₁ 72.33 (20.48) Cr ₂ 167.00 (17.60) I Cr ₁ 94.16 (–34.20) Cr ₂ 141.11 (–60.34) I
6b	Cr ₁ 107.25 (17.20) Cr ₂ 171.16 (35.21) I Cr ₁ 98.80 (–23.10) Cr ₂ 152.00 (–15.49) I
7b	Cr ₁ 95.20 (18.22) Cr ₂ 176.22 (30.18) I Cr ₁ 87.70 (–16.60) Cr ₂ 158.20 (–42.73) I
1c	Cr 134.31 (19.30) SmA 152.22 (0.87) I Cr 132.19 (–20.38) SmA 148.00 (–1.29) I
2c	Cr 140.20 (26.94) SmA 157.44 (2.69) I Cr 135.80 (–34.70) SmA 152.03 (–1.64) I
3c	Cr 149.38 (14.48) N 166.59 (1.63) I Cr 140.18 (–20.60) N 163.00 (–1.77) I
4c	Cr 155.06 (16.85) N 171.54 (1.69) I Cr 150.27 (–12.17) N 166.58 (–1.40) I
5c	Cr 153.55 (31.53) N 178.60 (2.40) I Cr 156.00 (–16.40) N 172.10 (–0.80) I
6c	Cr 167.29 (23.16) N 184.33 (2.66) I Cr 157.20 (–27.37) N 178.30 (–1.38) I
7c	Cr 176.60 (14.89) N 193.50 (1.28) I Cr 169.52 (–21.46) N 188.30 (–1.66) I

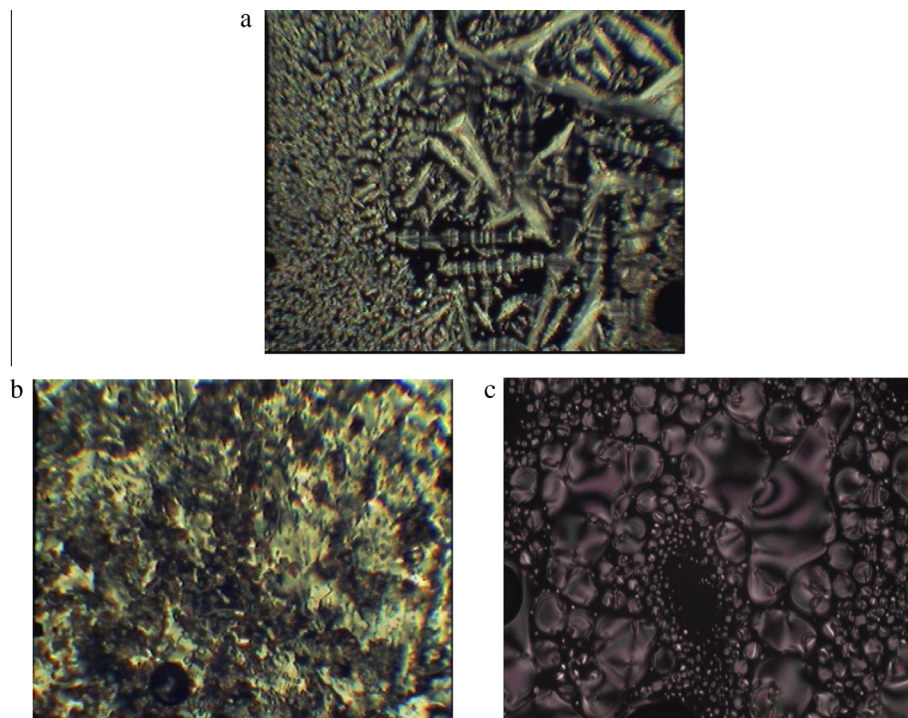


Fig. 1. (a) Optical photomicrograph for compound **2c** which exhibit fan-shaped texture of SmA phase upon cooling at 158.23 °C; (b) optical photomicrograph for compound **5c** which exhibit N phase upon heating at 174.55 °C; and (c) optical photomicrograph of compound **5c** upon cooling the small droplets coalesced to form the marble texture of the N phase at 167.28 °C.

on a Bruker 400 MHz Ultrashield™ FT-NMR spectrometer equipped with a 5 mm BBI inverse gradient probe. Chemical shifts were referenced to an internal TMS. The concentration of solute molecules was 50 mg in 1.0 mL DMSO. Standard Bruker pulse programs [20] were used throughout the entire experiment.

The phase transition temperatures and enthalpy values were measured by Perkin Elmer Pyris 1 DSC at a heating and cooling rate of 5 °C min⁻¹.

The textures were observed using a Carl Zeiss Axioskop 40 polarizing microscope equipped with a Mettler FP5 hot stage and TMS94 temperature controller. The samples studied by optical microscopy were prepared as a thin film sandwiched between glass slides and a cover.

The theoretical study was performed using HyperChem 8.0.8 in the liquid crystal institute of Kent state University USA.

Results and discussion

Phase transition and mesomorphic behaviour of compounds **1a–7a**, **1b–7b** and **1c–7c**

The transition temperatures and associated enthalpies upon the heating and cooling processes are listed in Table 2. Upon heating and cooling the DSC thermogram of compounds **1a–4a** showed two peaks. The first peak which was observed upon heating at the respective temperatures of 128.18 °C ($\Delta H = 31.68$ kJ mol⁻¹), 134.74 °C ($\Delta H = 68.11$ kJ mol⁻¹), 139.26 °C ($\Delta H = 55.29$ kJ mol⁻¹), and 148.37 °C ($\Delta H = 25.69$ kJ mol⁻¹), are characteristic of direct isotropization (Cr₁–I). The peak at temperatures 71.20 °C ($\Delta H = -28.34$ kJ mol⁻¹), 76.50 °C ($\Delta H = -42.22$ kJ mol⁻¹), 84.48 °C ($\Delta H = -17.69$ kJ mol⁻¹) and 93.72 °C ($\Delta H = -31.07$ kJ mol⁻¹) are characteristic of crystallization (I–Cr₁) upon cooling.

The Cr₁–Cr₂ transition which was observed for compounds **5a**, **6a** and **7a** with a long terminal chain can be shown under polarized light and by a DSC thermogram.

The compounds **1b–7b** are a good example of an homologous series with a different heterocyclic ring. Analysis by DSC and POM reveal that the new compounds are not mesogenic. Based on the DSC thermograms, the peaks which are observed upon heating of all compounds **1b–7b** at the temperatures of 65.19 °C ($\Delta H = 29.00$ kJ mol⁻¹), 140.10 °C ($\Delta H = 80.23$ kJ mol⁻¹), 81.10 °C ($\Delta H = 50.37$), 146.80 °C ($\Delta H = 30.24$ kJ mol⁻¹), 94.34 °C ($\Delta H = 42.31$), 156.27 °C ($\Delta H = 13.70$ kJ mol⁻¹) and 87.30 °C ($\Delta H = 18.50$ kJ mol⁻¹) are assigned to the phase transition of Cr₁–Cr₂. The peak which was observed at the temperatures of 163.20 °C ($\Delta H = 20.57$ kJ mol⁻¹), 72.33 °C ($\Delta H = 20.48$ kJ mol⁻¹), 167 °C ($\Delta H = 17.60$ kJ mol⁻¹), 107.25 °C ($\Delta H = 17.20$ kJ mol⁻¹), 171.16 °C ($\Delta H = 35.21$ kJ mol⁻¹), 95.20 °C ($\Delta H = 18.22$ kJ mol⁻¹) and 176.22 °C ($\Delta H = 30.18$ kJ mol⁻¹) for the respective compounds **1b–7b** show the transition Cr₂–I. Likewise, the phase sequence of Iso–Cr₂–Cr₁ was also observed on cooling run (Table 2). The texture observed under POM is indicative of the presence of sub-phases within the crystal phase (Cr₁–Cr₂), which resembled the phenomena reported in literature [16–18,21,22]. The clearing temperatures increased as the number of carbon atoms in the alkoxy chains increased (Fig. 3a). This can probably be attributed to an enhanced dispersive interaction or Van der Waals interaction between the terminal alkoxy chains and the oxazepandione ring [23].

In the compound series **1c–7c**, the change in the alkoxy chain length showed a strong effect on phase transition. Compounds **1c** and **2c**, with hexyloxy or octyloxy chains, exhibit a SmA phase upon heating and cooling. The heating cycle of the polarizing optical microscopy (POM) showed the formation of batonnets that coalesced to form a focal conic fan-shaped texture, something which is characteristic of SmA (Fig. 1a). The peaks observed during the heating cycle of the DSC thermogram at temperatures of 152.22 °C ($\Delta H = 0.87$ kJ mol⁻¹) and 157.44 °C ($\Delta H = 2.69$ kJ mol⁻¹) are related to the SmA–I phase (Fig. 2a). The temperature ranges of the mesophase upon heating cycle are found to be relatively wide (17.91 °C and 17.24 °C) compared with our

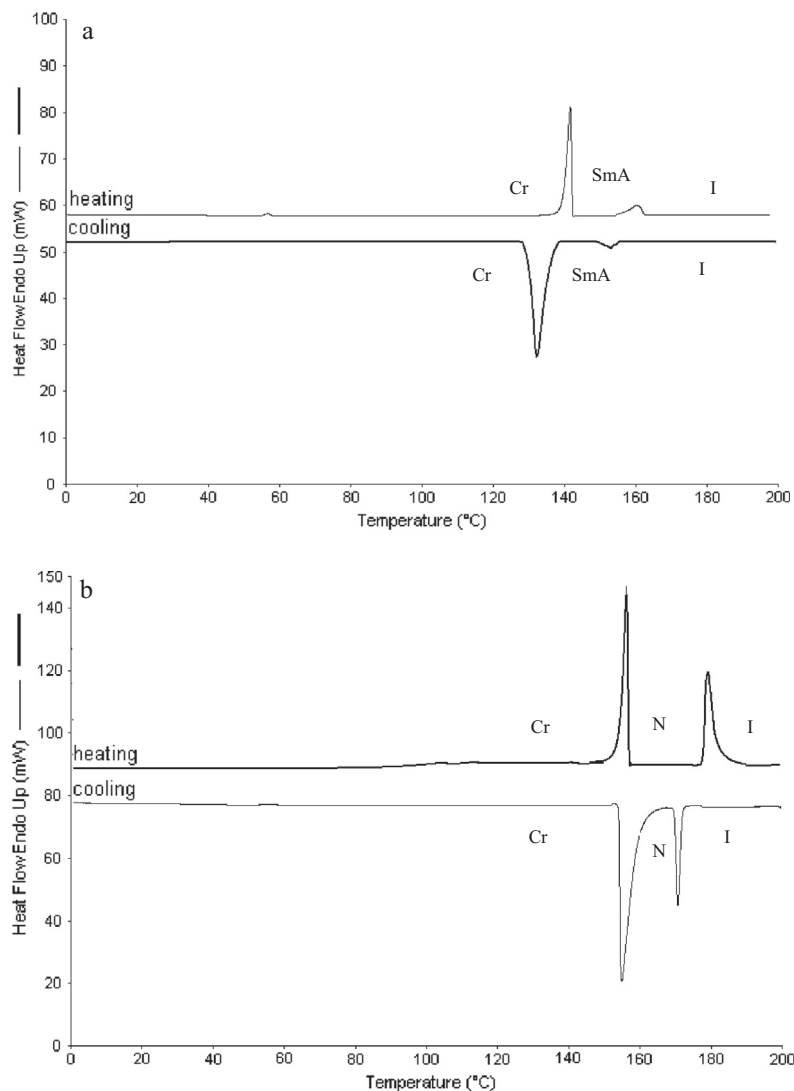


Fig. 2. DSC thermograms plot on heating and cooling for selected compounds (a) **2c** and (b) **5c**.

previous study [17,18]. The cooling of isotropic liquids of compounds **1c** and **2c** led to the initial formation of short rods (batonnets), which thereafter coalesced to a classic focal conic fan-shaped texture, something which is characteristic of the SmA phase (Fig. 1a). The I-SmA phase was also observed during the cooling run on the DSC thermogram at temperatures of 148 °C ($\Delta H = -1.29 \text{ kJ mol}^{-1}$) and 152.03 °C ($\Delta H = -1.64 \text{ kJ mol}^{-1}$), for respective compounds **1c** and **2c**. The temperature ranges of the mesophase upon heating are 15.81 °C and 16.23 °C.

The nematic phase was observed in homologues compounds **3c–7c**, in which the number of carbon atoms in the alkyloxy chains is $n \geq 10$. The texture observed under polarizing optical microscopy (POM) during the heating scan showed the presence of Schlieren texture characteristics of the nematic phase (Fig. 1b). The DSC thermogram also revealed the N–I phase transition by the peaks observed during the heating cycle at the temperatures of 166.59 °C ($\Delta H = 4.63 \text{ kJ mol}^{-1}$), 171.54 °C ($\Delta H = 1.69 \text{ kJ mol}^{-1}$), 178.60 °C ($\Delta H = 5.40 \text{ kJ mol}^{-1}$), 184.33 °C ($\Delta H = 7.66 \text{ kJ mol}^{-1}$) and 193.50 °C ($\Delta H = 1.28 \text{ kJ mol}^{-1}$) for compounds **3c–7c**, respectively and with the temperature ranges of the mesophase (17.21 °C, 16.48 °C, 25.05 °C, 17.14 °C and 16.90 °C). Upon cooling of the isotropic liquid in compounds **3c–7c**, a small droplet appeared and coalesced to form the classical or marbled texture,

which is characteristic of a nematic phase (Fig. 1b). Inspection of the DSC data further suggests that the temperature ranges of mesophase upon cooling are found to be relatively wide (23.40 °C, 16.31 °C, 16.10 °C, 21.10 °C and 18.78 °C for **3c**, **4c**, **5c**, **6c** and **7c**, respectively), compared with other compounds having the same heterocyclic ring in our previous study [17].

The effects of the terminal alkoxy chains with mesomorphic properties can be established by plotting graphs of phase transition temperatures against the number of carbons in the alkoxy chains (during heating and cooling cycles). According to Fig. 3b, the effect is noticed in short ($n = 6$ and 8) length of alkoxy chains where the SmA is observed. As the length of the carbon alkoxy chains increases, the nematic phase is observed for the compounds (**3c**, **4c**, **5c**, **6c** and **7c**). The nematogenic behaviour between compounds **3c–7c** suggested that when the carbon chains reached a certain length ($n \geq 10$), the nematic phase at the higher temperatures is induced [24]. Conversely, Fig. 3b showed that the melting point increased as the number of carbons in the terminal alkoxy chains increased, with the melting temperatures very clearly increasing from $n = 6$ to 18 [25]. This may be due to the excessive Van der Waals attractive forces between the long alkoxy chains.

Theoretical studies are also in agreement with these experimental results. The presence of a benzene ring adjacent to

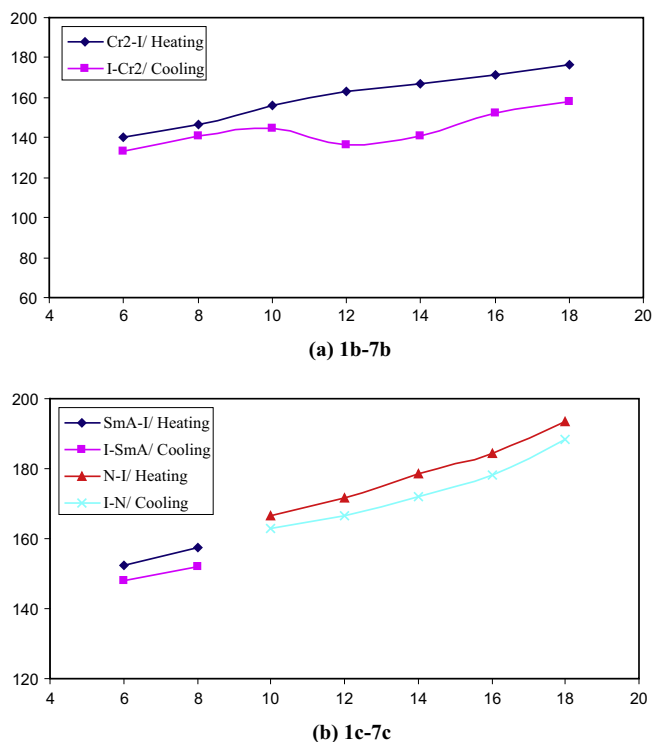


Fig. 3. The dependence of phase transition temperatures, T on the number of methylene in (a) compounds **1b–7b** and (b) compounds **1c–7c**.

the seven-membered ring (compounds type c) affords the molecules more flexibility compared with compounds of type a and b (Fig. 4).

In previous papers, we had reported that the emergence of mesomorphic properties of compounds with oxazepinediones seemed to be suppressed during the heating and cooling cycles [16,17]. However, the introduction of the terminal alkoxy chains

as reported here for the series of compounds **1c–7c** has enhanced the liquid crystallinity of these compounds, leading to a mesophase containing SmA and N phases.

Physical characterization

Characterization by FT-IR spectroscopy

FTIR data for compounds **1a–7a**, **1b–7b** and **1c–7c** are tabulated in Table 3. The stretching of the lactone and lactam carbonyl groups can be substantiated by the strong absorption band observed at the frequency range of $1711–1732\text{ cm}^{-1}$. The diagnostic bands due to the stretching of aliphatic C–H are shown within

Table 3
FTIR spectral data (cm^{-1}) of compounds **1a–7a**, **1b–7b** and **1c–7c** in solid state (embedded in KBr).

Compounds	$\nu(\text{C–H})_{\text{aliphatic}}$	$\nu(\text{C=C})_{\text{aromatic}}$	$\nu(\text{C=O})_{\text{lactam, lactone}}$		$\nu(\text{C}_4\text{O})$
1a	2977, 2930, 2870 and 2820	1602, 1567	1720	1240	
2a	2966, 2920, 2862 and 2800	1605, 1577	1732	1248	
3a	2970, 2930, 2865 and 2805	1600, 1575	1727	1245	
4a	2962, 2928, 2859 and 2802	1602, 1568	1730	1250	
5a	2960, 2922, 2861 and 2819	1604, 1564	1728	1254	
6a	2970, 2925, 2862 and 2821	1600, 1585	1730	1250	
7a	2964, 2928, 2870 and 2826	1605, 1580	1728	1247	
1b	2968, 2923, 2869 and 2824	1601, 1582	1730	1254	
2b	2972, 2923, 2866 and 2826	1604, 1581	1727	1253	
3b	2977, 2930, 2860 and 2829	1605, 1583	1730	1252	
4b	2970, 2926, 2864 and 2821	1604, 1583	1728	1253	
5b	2966, 2922, 2867 and 2822	1603, 1585	1729	1250	
6b	2968, 2920, 2860 and 2820	1601, 1580	1726	1254	
7b	2961, 2925, 2863 and 2821	1600, 1583	1728	1253	
1c	2966, 2926, 2860 and 2818	1605, 1580	1723	1259	
2c	2960, 2920, 2851 and 2830	1603, 1582	1712	1258	
3c	2958, 2920, 2850 and 2827	1604, 1580	1711	1256	
4c	2963, 2925, 2855 and 2821	1600, 1585	1722	1259	
5c	2960, 2921, 2843 and 2819	1605, 1582	1720	1252	
6c	2962, 2925, 2850 and 2820	1604, 1584	1722	1257	
7c	2964, 2922, 2853 and 2822	1602, 1582	1720	1258	

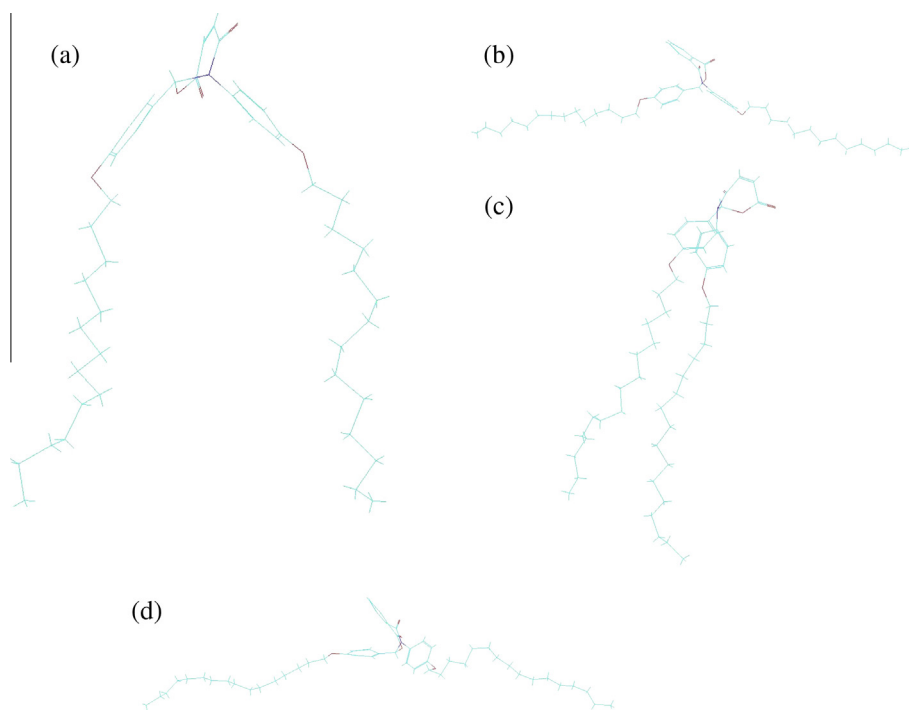


Fig. 4. Molecular models of (a) compound **5a**; (b) compound **5c**; (c) compound **6a**; and (d) compound **6c**, using HyperChem program.

Table 4a¹H NMR chemical shift (ppm) of compounds **1a–7a** and **1b–7b**.

Com.	H2 and H6	H3 and H5	H13 and H17	H14 and H16	H7	H9	H10	C ₄ –OCH ₂	C ₁₅ –OCH ₂	(CH ₂) _n	CH ₃
1a	7.61 (d, <i>J</i> = 8.18 Hz)	7.13 (d, <i>J</i> = 8.45 Hz)	7.88 (d, <i>J</i> = 8.01 Hz)	7.31 (d, <i>J</i> = 8.56 Hz)	9.80 s	6.26 (d, <i>J</i> = 12.70 Hz)	6.43 (d, <i>J</i> = 12.55 Hz)	4.09 t	4.01 t	1.73–1.21 m	0.89 t
2a	7.59 (d, <i>J</i> = 8.22 Hz)	7.12 (d, <i>J</i> = 8.43 Hz)	7.82 (d, <i>J</i> = 8.00 Hz)	7.30 (d, <i>J</i> = 8.60 Hz)	9.81 s	6.27 (d, <i>J</i> = 12.72 Hz)	6.42 (d, <i>J</i> = 12.50 Hz)	4.08 t	3.99 t	1.75–1.25 m	0.88 t
3a	7.64 (d, <i>J</i> = 8.14 Hz)	7.10 (d, <i>J</i> = 8.40 Hz)	7.85 (d, <i>J</i> = 8.08 Hz)	7.33 (d, <i>J</i> = 8.57 Hz)	9.81 s	6.25 (d, <i>J</i> = 12.73 Hz)	6.44 (d, <i>J</i> = 12.59 Hz)	4.08 t	3.98 t	1.73–1.20 m	0.89 t
4a	7.71 (d, <i>J</i> = 8.19 Hz)	7.14 (d, <i>J</i> = 8.39 Hz)	7.80 (d, <i>J</i> = 7.95 Hz)	7.34 (d, <i>J</i> = 8.53 Hz)	9.82 s	6.28 (d, <i>J</i> = 12.70 Hz)	6.44 (d, <i>J</i> = 12.53 Hz)	4.07 t	4.02 t	1.77–1.23 m	0.89 t
5a	7.65 (d, <i>J</i> = 8.21 Hz)	7.18 (d, <i>J</i> = 8.35 Hz)	7.89 (d, <i>J</i> = 7.90 Hz)	7.35 (d, <i>J</i> = 8.62 Hz)	9.82 s	6.26 (d, <i>J</i> = 12.74 Hz)	6.46 (d, <i>J</i> = 12.51 Hz)	4.09 t	3.98 t	1.76–1.20 m	0.88 t
6a	7.70 (d, <i>J</i> = 8.19 Hz)	7.13 (d, <i>J</i> = 8.39 Hz)	7.88 (d, <i>J</i> = 8.03 Hz)	7.31 (d, <i>J</i> = 8.49 Hz)	9.85 s	6.25 (d, <i>J</i> = 12.72 Hz)	6.45 (d, <i>J</i> = 12.49 Hz)	4.09 t	3.97 t	1.74–1.24 m	0.87 t
7a	7.69 (d, <i>J</i> = 8.20 Hz)	7.10 (d, <i>J</i> = 8.41 Hz)	7.83 (d, <i>J</i> = 8.01 Hz)	7.32 (d, <i>J</i> = 8.52 Hz)	9.84 s	6.27 (d, <i>J</i> = 12.72 Hz)	6.43 (d, <i>J</i> = 12.60 Hz)	4.08 t	4.02 t	1.73–1.25 m	0.86 t
1b	7.47 (d, <i>J</i> = 8.80 Hz)	7.25 (d, <i>J</i> = 8.44 Hz)	7.72 (d, <i>J</i> = 8.33 Hz)	7.31 (d, <i>J</i> = 8.77 Hz)	9.85 s	2.25 (t, <i>J</i> = 7.12 Hz)	2.44 (t, <i>J</i> = 7.25 Hz)	4.08 t	4.01 t	1.74–1.26 m	0.89 t
2b	7.46 (d, <i>J</i> = 8.82 Hz)	7.23 (d, <i>J</i> = 8.43 Hz)	7.70 (d, <i>J</i> = 8.31 Hz)	7.31 (d, <i>J</i> = 8.70 Hz)	9.85 s	2.28 (t, <i>J</i> = 7.11 Hz)	2.46 (t, <i>J</i> = 7.29 Hz)	4.08 t	4.00 t	1.73–1.25 m	0.88 t
3b	7.49 (d, <i>J</i> = 8.83 Hz)	7.23 (d, <i>J</i> = 8.42 Hz)	7.71 (d, <i>J</i> = 8.32 Hz)	7.34 (d, <i>J</i> = 8.75 Hz)	9.87 s	2.27 (t, <i>J</i> = 7.10 Hz)	2.47 (t, <i>J</i> = 7.28 Hz)	4.09 t	4.01 t	1.72–1.21 m	0.89 t
4b	7.45 (d, <i>J</i> = 8.85 Hz)	7.28 (d, <i>J</i> = 8.48 Hz)	7.72 (d, <i>J</i> = 8.30 Hz)	7.32 (d, <i>J</i> = 8.71 Hz)	9.88 s	2.28 (t, <i>J</i> = 7.13 Hz)	2.45 (t, <i>J</i> = 7.26 Hz)	4.07 t	4.00 t	1.75–1.25 m	0.88 t
5b	7.44 (d, <i>J</i> = 8.87 Hz)	7.29 (d, <i>J</i> = 8.40 Hz)	7.71 (d, <i>J</i> = 8.33 Hz)	7.32 (d, <i>J</i> = 8.73 Hz)	9.85 s	2.25 (t, <i>J</i> = 7.14 Hz)	2.44 (t, <i>J</i> = 7.24 Hz)	4.08 t	4.02 t	1.77–1.26 m	0.88 t
6b	7.46 (d, <i>J</i> = 8.88 Hz)	7.20 (d, <i>J</i> = 8.41 Hz)	7.70 (d, <i>J</i> = 8.31 Hz)	7.34 (d, <i>J</i> = 8.70 Hz)	9.86 s	2.27 (t, <i>J</i> = 7.18 Hz)	2.43 (t, <i>J</i> = 7.28 Hz)	4.09 t	4.01 t	1.74–1.24 m	0.89 t
7b	7.47 (d, <i>J</i> = 8.86 Hz)	7.27 (d, <i>J</i> = 8.47 Hz)	7.72 (d, <i>J</i> = 8.30 Hz)	7.31 (d, <i>J</i> = 8.77 Hz)	9.84 s	2.28 (t, <i>J</i> = 7.11 Hz)	2.44 (t, <i>J</i> = 7.25 Hz)	4.08 t	4.00 t	1.75–1.26 m	0.87 t

Table 4b¹H NMR chemical shift (ppm) of compounds **1c–7c**.

Com.	H2 and H6	H3 and H5	H17 and H21	H18 and H20	H7	H12	H13	H14	H15	C ₄ –OCH ₂	C ₁₉ –OCH ₂	(CH ₂) _n	CH ₃
1c	7.42 (d, <i>J</i> = 8.50 Hz)	7.14 (d, <i>J</i> = 8.29 Hz)	7.78 (d, <i>J</i> = 8.30 Hz)	7.41 (d, <i>J</i> = 8.40 Hz)	9.80 s	8.10 (d, <i>J</i> = 8.01 Hz)	7.52 (t, <i>J</i> = 7.98 Hz)	7.60 (t, <i>J</i> = 8.42 Hz)	7.35 (d, <i>J</i> = 8.31 Hz)	4.16 t	4.02 t	1.78–1.24 m	0.88 t
2c	7.40 (d, <i>J</i> = 8.55 Hz)	7.12 (d, <i>J</i> = 8.28 Hz)	7.71 (d, <i>J</i> = 8.32 Hz)	7.40 (d, <i>J</i> = 8.40 Hz)	9.81 s	8.09 (d, <i>J</i> = 8.09 Hz)	7.51 (t, <i>J</i> = 7.97 Hz)	7.62 (t, <i>J</i> = 8.41 Hz)	7.36 (d, <i>J</i> = 8.33 Hz)	4.15 t	4.02 t	1.79–1.24 m	0.87 t
3c	7.44 (d, <i>J</i> = 8.39 Hz)	7.19 (d, <i>J</i> = 8.28 Hz)	7.73 (d, <i>J</i> = 8.36 Hz)	7.41 (d, <i>J</i> = 8.42 Hz)	9.82 s	8.08 (d, <i>J</i> = 8.00 Hz)	7.50 (t, <i>J</i> = 7.88 Hz)	7.63 (t, <i>J</i> = 8.40 Hz)	7.36 (d, <i>J</i> = 8.22 Hz)	4.16 t	4.00 t	1.77–1.24 m	0.88 t
4c	7.42 (d, <i>J</i> = 8.53 Hz)	7.17 (d, <i>J</i> = 8.27 Hz)	7.75 (d, <i>J</i> = 8.33 Hz)	7.43 (d, <i>J</i> = 8.40 Hz)	9.82 s	8.12 (d, <i>J</i> = 8.09 Hz)	7.52 (t, <i>J</i> = 7.93 Hz)	7.61 (t, <i>J</i> = 8.47 Hz)	7.31 (d, <i>J</i> = 8.29 Hz)	4.16 t	4.02 t	1.78–1.27 m	0.88 t
5c	7.44 (d, <i>J</i> = 8.54 Hz)	7.18 (d, <i>J</i> = 8.29 Hz)	7.70 (d, <i>J</i> = 8.31 Hz)	7.41 (d, <i>J</i> = 8.42 Hz)	9.81 s	8.11 (d, <i>J</i> = 8.02 Hz)	7.54 (t, <i>J</i> = 7.98 Hz)	7.63 (t, <i>J</i> = 8.43 Hz)	7.30 (d, <i>J</i> = 8.22 Hz)	4.13 t	4.01 t	1.79–1.26 m	0.89 t
6c	7.42 (d, <i>J</i> = 8.55 Hz)	7.13 (d, <i>J</i> = 8.29 Hz)	7.74 (d, <i>J</i> = 8.36 Hz)	7.39 (d, <i>J</i> = 8.44 Hz)	9.82 s	8.10 (d, <i>J</i> = 8.04 Hz)	7.52 (t, <i>J</i> = 7.92 Hz)	7.62 (t, <i>J</i> = 8.40 Hz)	7.35 (d, <i>J</i> = 8.26 Hz)	4.16 t	4.00 t	1.78–1.24 m	0.88 t
7c	7.42 (d, <i>J</i> = 8.57 Hz)	7.11 (d, <i>J</i> = 8.30 Hz)	7.73 (d, <i>J</i> = 8.37 Hz)	7.40 (d, <i>J</i> = 8.41 Hz)	9.80 s	8.08 (d, <i>J</i> = 8.10 Hz)	7.50 (t, <i>J</i> = 7.93 Hz)	7.64 (t, <i>J</i> = 8.46 Hz)	7.36 (d, <i>J</i> = 8.30 Hz)	4.17 t	4.00 t	1.77–1.22 m	0.89 t

2800–2977 cm^{-1} range. This value conforms to that reported by Yeap et al. [16]. The appearance of strong absorption bands within 1564–1605 cm^{-1} is attributable to the stretching of the C=C of the aromatic ring. Absorption bands observed in the 1240–1259 cm^{-1} range is assignable to the stretching of the ether linkages.

Characterization by NMR spectra

A complete assignment for the title compounds can be performed by relating the data to the respective compounds as shown in Scheme 1, in which three types of compounds have been differentiated by **a**, **b** and **c**. The ^1H NMR spectra of compounds **1a–7a** indicate that the aromatic protons with different chemical shifts ranging from $\delta = 7.10$ to 7.88 ppm are observed as four doublets. The presence of a singlet within the frequency range of $\delta = 9.80$ –9.88 ppm can be attributed to the H7 atom in the heterocyclic ring. This can be further substantiated by the direct bond heteronuclear correlation with C7 within the frequency range of $\delta = 88.83$ –89.03 ppm. The presence of two doublets in the downfield region of $\delta = 6.25$ –6.28 ppm and $\delta = 6.42$ –6.47 ppm for compounds **1a–7a** can be attributed to H9 and H10 of the heterocyclic ring. This is an indication of intramolecular cyclization of compounds **1a–7a**. Likewise, the resonances for the aromatic protons of compounds **1b–7b** appear as four doublets in the downfield region of $\delta = 7.44$ –7.49 ppm, $\delta = 7.20$ –7.29 ppm, $\delta = 7.70$ –7.72 ppm and $\delta = 7.31$ –7.34 ppm corresponding to the respective phenyl protons H2 (or H6), H3 (or H5), H13 (or H17) and H14 (or H16) in compounds **1b–7b**. The ^1H NMR spectra of compounds **1b–7b** indicate that the H9 and H10 protons from the heterocyclic ring appear as two triplets in the range of $\delta = 2.25$ –2.28 ppm and $\delta = 2.43$ –2.47 ppm, respectively. The H7 proton appears as a singlet at $\delta = 9.84$ –9.88. The ^1H NMR data for compounds **1c–7c** showed diagnostic signals within the range of $\delta = 7.11$ –8.12 ppm which is assignable to the aromatic protons. The ^1H NMR spectra of the title compounds **1c–7c** showed a singlet which shows an integration of one hydrogen at chemical shift $\delta = 9.80$ –9.82 ppm which corresponds to the proton attached to the carbon C7 in heterocyclic ring.

The same ^1H NMR spectra also showed signals for aliphatic protons. These signals are assigned with the aid of the COSY experiment. The sets of multiplets within the frequency range of $\delta = 1.20$ –1.77 ppm can be assigned to the presence of methylene protons, $\text{OCH}_2\text{CH}_2(\text{CH}_2)_n$ where n is the number of carbon atoms in both terminal chains. Signals attributable to the presence of methylene protons (C_4 – OCH_2 , C_{15} – OCH_2 and C_{19} – OCH_2 of the ether linking groups), are observed at chemical shifts ranging from $\delta = 4.07$ –4.17, $\delta = 3.98$ –4.02 and $\delta = 4.00$ –4.02 ppm, respectively. These values conform to those reported by Yeap et al. [4,13]. Triplets observed within the frequency range of $\delta = 0.86$ –0.89 ppm can be assigned to the methyl protons (CH_3) of both terminal alkyl chains (Tables 4a and 4b).

The structures of the title compounds are further substantiated by ^{13}C NMR spectroscopic data. The ^{13}C NMR spectra of compounds **1a–7a**, **1b–7b** and **1c–7c** indicate the presence of aromatic carbons with peaks within the frequency range of $\delta = 116.09$ –164.11 ppm. The aromatic carbons and quaternary carbons are assigned with the aid of an HMBC experiment. The C2 (or C6) and C3 (or C5) are assigned, respectively, at $\delta = 124.05$ –126.69 and $\delta = 116.09$ –116.95 based on their correlations with H3 (or H5) and H2 (or H6). The correlation between H16 (or H14), H13 (or H17) and C13 (or C17), C16 (or C14) are used to assign the chemical shift of the latter at $\delta = 132.23$ –132.94 and $\delta = 130.26$ –130.60 ppm in respective compounds of type **a** and **b**. In compounds of type **c**, the correlation between H18 (or H20), H17 (or H20), and C17 (or C21), C18 (or C20) were also used to assign the chemical shift at $\delta = 134.09$ –134.90 ppm and $\delta = 130.19$ –130.50 ppm. The assignment of C7 at $\delta = 88.90$ –90.93 ppm is based on its correlation with the H2 (or H6) atom for each member of the three homologous series. The C9 and C10 signals in homologous series **a** and **b** are observed at $\delta = 133.80$ –133.90 ppm, $\delta = 30.60$ –30.69 ppm, $\delta = 130.05$ –130.09 ppm and $\delta = 28.01$ –28.08 ppm, respectively, based on its correlation with H9 and H10. The HMBC spectra also showed a cross peak of the C12 atom with the H15 atom at $\delta = 127.09$ –127.88 ppm in compound series **c** (see Table 5)

Table 5
 ^{13}C NMR chemical shift (ppm) of compounds **1a–7a**, **1b–7b** and **1c–7c**.

Com.	C1	C2, C6	C4	C3, C5	C7	C8	C9	C10	C11	C13, C17	C14, C16	C ₄ –OCH ₂	C ₁₉ –OCH ₂	(CH ₂) _n	CH ₃	
1a	130.10	126.61	161.21	116.92	88.91	170.11	133.86	130.08	172.74	132.28	130.33	68.20	69.17	21.59–33.60	15.90	
2a	130.17	126.60	161.22	116.91	88.89	170.13	133.87	130.07	172.70	132.23	130.39	68.21	69.22	21.49–33.30	15.88	
3a	130.11	126.63	161.20	116.94	88.94	170.16	133.80	130.05	172.74	132.29	130.41	68.16	69.72	21.41–33.49	15.09	
4a	130.16	126.66	161.22	116.90	88.83	170.19	133.80	130.06	172.69	132.30	130.37	68.16	69.59	22.20–32.90	15.28	
5a	130.19	126.68	161.25	116.95	88.92	170.16	133.82	130.05	172.77	132.29	130.43	68.22	69.32	23.70–32.60	15.10	
6a	130.13	126.60	161.29	116.88	88.97	170.14	133.89	130.09	172.71	132.31	130.44	68.26	69.44	22.90–33.20	14.90	
7a	130.16	126.69	161.30	116.96	88.90	170.19	133.90	130.08	172.89	132.28	130.47	68.30	69.57	22.77–32.98	15.66	
1b	130.18	126.67	161.29	116.90	89.03	173.32	30.69	28.01	176.93	132.88	130.26	68.33	69.49	23.01–33.08	15.41	
2b	130.19	126.68	161.23	116.94	89.03	173.30	30.66	28.02	176.90	132.70	130.29	68.29	69.50	23.60–31.18	15.51	
3b	130.16	126.60	161.27	116.93	88.95	173.32	30.65	28.01	177.01	132.94	130.38	68.26	69.50	23.03–31.90	15.22	
4b	130.14	126.63	161.21	116.98	88.97	173.37	30.67	28.02	177.01	132.79	130.57	68.30	69.19	23.29–31.80	15.15	
5b	130.19	126.60	161.28	116.94	88.93	173.39	30.63	28.04	177.10	132.88	130.55	68.28	69.20	23.20–31.87	15.09	
6b	130.18	126.66	161.23	116.90	88.97	173.36	30.69	28.08	177.26	132.83	130.58	68.29	69.17	23.09–31.19	15.89	
7b	130.16	126.65	161.20	116.95	88.92	173.36	30.60	28.06	177.13	132.91	130.60	68.19	69.20	23.38–32.09	15.11	
Com.	C1	C2, C6	C4	C3, C5	C7	C8	C9	C10	C11	C12	C17, C21	C18, C20	C ₄ –OCH ₂	C ₁₉ –OCH ₂	(CH ₂) _n	CH ₃
1c	131.01	124.26	164.09	116.09	90.01	171.90	131.01	129.90	167.03	127.50	134.11	130.22	68.66	70.22	24.44–34.09	15.00
2c	131.66	124.09	164.18	116.14	90.26	171.91	131.51	129.89	167.90	127.51	134.90	130.26	68.60	70.03	24.93–34.12	15.04
3c	131.19	124.33	164.99	116.89	90.33	171.80	131.67	129.40	167.50	127.51	134.50	130.50	68.51	70.55	24.11–34.34	15.04
4c	131.29	124.90	164.81	116.77	90.82	171.20	131.89	129.22	167.12	127.09	134.22	130.44	68.22	70.56	24.01–34.51	15.11
5c	131.33	124.05	164.11	116.50	90.79	171.11	131.77	129.51	167.22	127.11	134.09	130.50	68.78	70.44	24.55–34.90	15.25
6c	131.09	124.14	164.27	116.28	90.47	171.10	131.09	129.61	167.89	127.75	134.50	130.19	68.67	70.21	24.27–34.71	15.41
7c	131.01	124.58	164.69	116.33	90.93	171.33	131.28	129.33	167.90	127.88	134.22	130.20	68.66	70.09	24.02–34.42	15.09

The correlation between H9 and H19 with C8 and C11 were used to assign the chemical shift of the carbonyl group at $\delta = 170.11\text{--}173.39$ ppm and $\delta = 172.69\text{--}177.26$ ppm in respective compounds **a** and **b**. Moreover, diagnostic peaks observed within the range $\delta = 171.10\text{--}171.91$ ppm and $\delta = 167.03\text{--}167.90$ ppm can be attributed to the presence of carbonyl groups (C=O) C8 and C9 in respective compounds **c**. Signals at $\delta = 68.16\text{--}68.78$ ppm and $\delta = 69.17\text{--}70.56$ ppm indicate the presence of the C–O group from the ether linkages. Signals attributable to the methylene carbons of the terminal alkyloxy chains are observed within the range of $\delta = 21.41\text{--}34.90$ ppm. Signals due to the methyl carbons are observed within the range of $\delta = 14.90\text{--}15.90$ ppm.

Conclusion

In this paper, the synthesis and liquid crystalline behaviour of the three series of heterocyclic rings with the terminal alkyloxy chains have been described. Compounds **1a–7a** are non-mesogenic and exhibit only I-Cr during heating and cooling, while the Cr₁–Cr₂ transition was observed for compounds **5a** to **7a**. All compounds **1b–7b** with oxazepanediones are non-mesogenic and only exhibit Cr₁–Cr₂ upon heating and cooling. However, the SmA and N phases were observed in series compounds **1c–7c**. The study also revealed that the length of the alkyl chain produces a significant effect on the liquid crystalline properties whereby the nematic phase can only be observed in compounds **1c–7c** for long-chain derivatives. Theoretical studies are in agreement with the experimental result.

Acknowledgements

The main author would like to thank Professor John. West and the Liquid Crystal Institute at Kent State University for performing

theoretical studies. The authors would also like to thank Universiti Sains Malaysia for supporting this project.

References

- [1] G.W. Gray, *Thermotropic Liquid Crystals*, John Wiley & Sons, New York, 1987.
- [2] C.H. Lee, T. Yamamoto, *Tetrahedron Lett.* 42 (2001) 3993.
- [3] J. Han, X.Y. Chang, Y.M. Wang, M.L. Pang, J.B. Meng, *J. Mol. Struct.* 937 (2009) 122.
- [4] G.Y. Yeap, W.S. Yam, L. Dobrzyski, E. Gorecka, D. Takeuchi, P.L. Boey, W.A.K. Mahmood, M.M. Ito, *J. Mol. Struct.* 937 (2009) 16.
- [5] D. Srividhya, S. Manjunathan, S. Thirumaran, C. Saravanan, S. Senthil, *J. Mol. Struct.* 937 (2009) 7.
- [6] A.A. Vieira, R. Cristiano, A.J. Bortoluzzi, H. Gallardo, *J. Mol. Struct.* 875 (2008) 364.
- [7] W.J. Lo, Y.L. Hong, R.H. Lin, J.L. Hong, *Mol. Cryst. Liq. Cryst.* 308 (1997) 133.
- [8] Y.H. Wang, Y.L. Hong, F.S. Yen, J.L. Hong, *Mol. Cryst. Liq. Cryst.* 287 (1996) 109.
- [9] D.J. Janietz, *Mater. Chem.* 8 (1998) 265.
- [10] D. Goldmann, D. Janietz, C. Schmidt, J.H. Wendorff, *Liq. Cryst.* 25 (1998) 711.
- [11] H. Kelker, R. Hatz, *Handbook of Liquid Crystals*, Verlag Chemie, Weinheim, 1980.
- [12] P.J. Collings, M. Hird, *Introduction to Liquid Crystals: Chemistry and Physics*, Taylor & Francis Ltd., UK, 1998.
- [13] A.S. Matharu, D.C. Asman, *Liq. Cryst.* 34 (2007) 1317.
- [14] H. Gallardo, R.F. Magnago, A.J. Bortoluzzi, *Liq. Cryst.* 28 (2001) 1343.
- [15] C.K. Lai, Y. Ke, J.S.C. Shen, W. Li, *Liq. Cryst.* 29 (2002) 915.
- [16] G.Y. Yeap, A.T. Mohammad, H. Osman, *J. Mol. Struct.* 982 (2010) 33.
- [17] G.Y. Yeap, A.T. Mohammad, H. Osman, *Mol. Cryst. Liq. Cryst.* 552 (2012) 177.
- [18] A.T. Mohammad, G.Y. Yeap, H. Osman, *Aust. J. Basic. Appl. Sci.* 5 (2011) 551.
- [19] Y. Tang, J.C. Fettinger, J.T. Shaw, *Org. Lett.* 11 (2009) 3802.
- [20] Bruker program 1D WIN-NMR (release 6.0) and 2D WIN-NMR (release 6.0).
- [21] G.Y. Yeap, S.T. Ha, P.L. Boey, W.A.K. Mahmood, M.M. Ito, S. Sanehisa, *Mol. Cryst. Liq. Cryst.* 73 (2004) 423.
- [22] J. Belmar, M. Parra, C. Zuniga, C. Perez, C. Munoz, A. Omenat, J.L. Serrano, *Liq. Cryst.* 26 (1999) 75.
- [23] W.S. Yam, G.Y. Yeap, *Chin. Chem. Lett.* 22 (2011) 229.
- [24] S.T. Ha, T.M. Koh, S.L. Lee, G.Y. Yeap, H.C. Lin, S.T. Ong, *Liq. Cryst.* 37 (2010) 547.
- [25] P.J. Collings, M. Hird, *Introduction to Liquid Crystals: Chemistry and Physics*, Taylor & Francis Ltd., London, 1998.